Is a Decline of AMOC Causing the Warming Hole above the North Atlantic in Observed and Modeled Warming Patterns?

SYBREN DRIJFHOUT, GEERT JAN VAN OLDENBORGH, AND ANDREA CIMATORIBUS

Royal Netherlands Meteorological Institute, De Bilt, Netherlands

ABSTRACT

The pattern of global mean temperature (GMT) change is calculated by regressing local surface air temperature (SAT) to GMT for an ensemble of CMIP5 models and for observations over the last 132 years. Calculations are based on the historical period and climate change scenarios. As in the observations the warming pattern contains a warming hole over the subpolar North Atlantic. Using a bivariate regression of SAT to GMT and an index of the Atlantic meridional overturning circulation (AMOC), the warming pattern is decomposed in a radiatively forced part and an AMOC fingerprint. The North Atlantic warming hole is associated with a decline of the AMOC. The AMOC fingerprint resembles Atlantic multidecadal variability (AMV), but details of the pattern change when the AMOC decline increases, underscoring the nonlinearity in the response.

The warming hole is situated south of deep convection sites, indicating that it involves an adjustment of the gyre circulation, although it should be noted that some models feature deep convection in the middle of the subpolar gyre. The warming hole is already prominent in historical runs, where the response of the AMOC to GMT is weak, which suggests that it is involved in an ocean adjustment that precedes the AMOC decline. In the more strongly forced scenario runs, the warming hole over the subpolar gyre becomes weaker, while cooling over the Nordic seas increases, consistent with previous findings that deep convection in the Labrador and Irminger Seas is more vulnerable to changes in external forcing than convection in the Nordic seas, which only reacts after a threshold is passed.

1. Introduction

In climate change scenarios the Atlantic meridional overturning circulation (AMOC) is projected to weaken during the twenty-first century in response to enhanced greenhouse gas forcing (Meehl et al. 2007). The associated cooling is expected to partly offset the greenhouse-induced warming in surface air temperature (SAT) over the North Atlantic. Woollings et al. (2012) show that a larger reduction in the AMOC is associated with greater cooling in the North Atlantic (their Fig. 1). Although the cooling features a marked spatial pattern, its uniform sign north of 20°N suggests that the response to an AMOC decline projects on Atlantic multidecadal variability (AMV) (Knight et al. 2005), underscoring the hypothesis that AMV is to a large extent driven by AMOC changes (Msadek and Frankignoul 2009; Latif and Keenlyside 2011). For instance, the correlation between AMOC and AMV on multidecadal to centennial time scales can exceed 0.8 in a coupled climate model (Wouters et al. 2012).

This implies that the AMV is not only the dominant pattern of observed detrended twentieth-century multidecadal SST anomalies; it also would project on the warming pattern of anthropogenically forced SAT insofar as a forced decline of the AMOC is involved. A calculation of the warming pattern of global mean temperature (GMT), by regressing observed SAT to GMT, reveals that at most places SAT and GMT are positively correlated. At some places, however, a negative regression coefficient arises, noticeably over the North Atlantic and North Pacific subpolar gyres. When the data are smoothed over decadal time scales, the negative regression over the North Atlantic becomes more prominent, while the area with negative regression coefficients over the North Pacific declines, suggesting different physical mechanisms at work. An increase of

Corresponding author address: Sybren Drijfhout, Royal Netherlands Meteorological Institute, P.O. Box 201, 3730AE De Bilt, Netherlands.
E-mail: drijfhou@knmi.nl
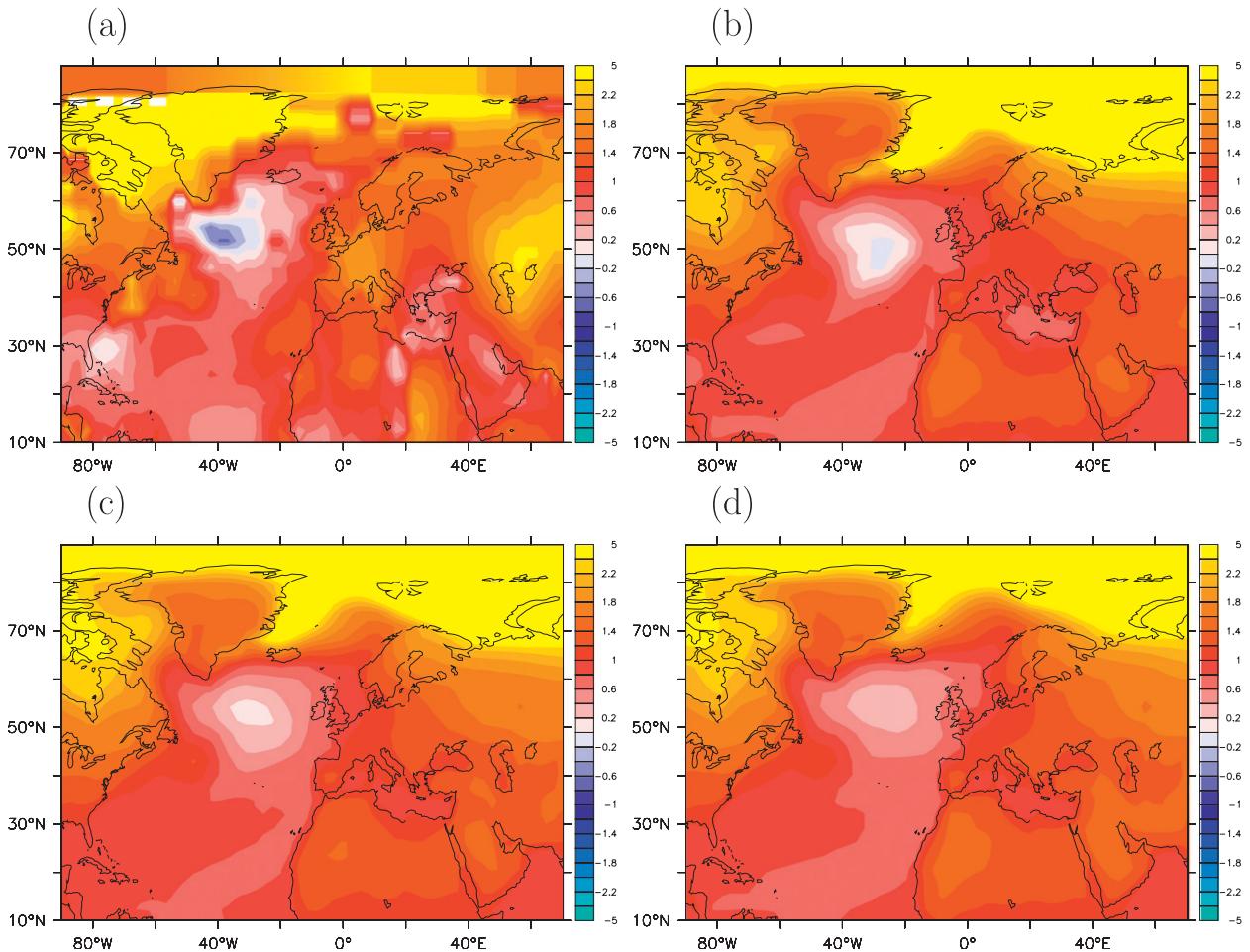
FIG. 1. Trend pattern of GMT in the North Atlantic sector, obtained by a univariate regression of SAT on GMT, for (a) observations, (b) historical runs, (c) the RCP 2.6 scenario, and (d) the RCP8.5 scenario.

the cooling over the North Atlantic when time scale increases is consistent with the hypothesis that the North Atlantic warming hole is associated with AMOC decline: the anthropogenically forced signals of AMOC decline and GMT rise correlate well, while the shorter-time natural fluctuations in AMOC and GMT do not. Figure 1a shows the regression of SAT on GMT for the observations in the North Atlantic sector after applying a decadal low-pass filter, highlighting the warming hole over the subpolar gyre.

In the following we show that the ensemble of phase 5 of the Coupled Model Intercomparison Project (CMIP5) features a similar North Atlantic warming hole in climate change scenarios and historical runs. In each scenario, the warming hole can be linked to a decline of the AMOC, but the fingerprint of AMOC decline changes for scenarios featuring stronger radiative forcing. In these scenarios cooling over the Nordic seas becomes more prominent. This paper is organized as follows. In section 2, we describe the data and the methodology used in this study. The results of the regression analysis are presented in section 3. Section 4 summarizes the main results.

2. Data and methodology

Climate model simulations from phase 5 of the World Climate Research Program's Coupled Model Intercomparison Project (Taylor et al. 2012) have been used and compared to observations from the Goddard Institute for Space Studies (GISS) surface temperature analysis (GISTEMP-1200) dataset (Hansen et al. 2010). For the CMIP5 analysis we used the historical runs, representing the late nineteenth and twentieth centuries, and the Representative Concentration Pathway (RDP) RCP2.6, RCP4.5, and RCP8.5 scenarios for the twenty-first century. Apart from SAT, meridional overturning streamfunction data were used. From these, an AMOC

index was calculated by averaging the AMOC strength between 500- and 2000-m depth and between the southern boundary of the Atlantic, around 34°S, and 50°N. In this way an index is obtained that optimally reflects large-scale changes in the AMOC associated with a long-term, anthropogenically forced trend, which indeed has a basin-scale expression (Drijfhout and Hazeleger 2007). At the same time the expression of natural AMOC variability is minimized, which is often characterized by a dipole pattern with a maximum amplitude near the AMOC maximum [see, e.g., Drijfhout and Hazeleger (2007) and Drijfhout et al. (2008) for a discussion of the relevant patterns].

The total number of models used is 12 (Table 1), determined by the availability of meridional overturning streamfunction data for the RCP2.6 scenario, which is less frequently simulated. The scenario runs and historical period were joined together, creating time series that are 240–251 years long. The period after 2100 was excluded to prevent one model getting to a high weight when the ensemble mean is calculated. Also, only one ensemble member was used for each model. In addition, the historical period was treated separately. For all models a univariate regression of SAT on GMT was performed by a simultaneous regression of all modeled SAT fields on GMT. That is, time series of all models were joined:

$$T(x, y, t, i) = A(x, y)T_{\text{global}}(t, i) + \varepsilon(x, y, t, i), \quad (1)$$

where $i = 1, \ldots, N$ is an index over the different models and $A(x, y)$ is the warming pattern.

Also, a bivariate regression of SAT on both GMT and the AMOC index was carried out:

$$T(x, y, t, i) = B(x, y)T_{\text{global}}(t, i) + C(x, y)\Psi(t, i) + \varepsilon(x, y, t, i), \quad (2)$$

where $B(x, y)$ is the radiatively forced pattern, $C(x, y)$ is the AMOC fingerprint, and Ψ is the AMOC index.

We performed lagged regressions as well because the response of SAT to AMOC variations is not instantaneous (Eden and Willebrand 2001), but since a variety of time scales is involved, all being model dependent, we discarded lagged regressions, as the regressions with zero lag generally gave the best results. Before performing the regression, at each point and in each model the time-averaged temperature and AMOC index was subtracted. The regression on the anomalies was performed with standard R routines.

TABLE 1. The regression of the AMOC-index on GMT in 10^6 m^3 s^{-1} K^{-1} for the 12 models of CMIP5 that were analyzed.

Model	Historical	RCP2.6	RCP4.5	RCP8.5
CanESM2	0.60	−0.80	−0.78	−0.72
CCSM4	−0.90	−1.44	−1.51	−1.52
CESM1-CAM5	−0.05	−2.23	−2.14	−1.81
CNRM-CM5	−0.98	−1.47	−1.24	−1.02
FGOALS-g2	0.35	−2.76	−2.16	−1.54
FGOALS-s2	−1.00	−3.00	−2.86	−2.03
GFDL-CM3	0.63	−2.84	−2.48	−2.11
GFDL-ESM2M	−1.37	−3.15	−3.13	−2.80
MPI-ESM-LR	−0.48	−1.53	−1.46	−1.17
MPI-ESM-MR	0.31	−1.03	−1.11	−1.00
MRI-CGCM3	−0.04	−0.88	−0.74	−0.92
NorESM1-M	0.89	−1.78	−1.88	−1.94
Ensemble mean	−0.4 ± 0.8	−1.9 ± 0.8	−1.8 ± 0.8	−1.5 ± 0.6

3. Regression patterns

The models' patterns of GMT change are shown in Figs. 1b–d for the historical period, the RCP2.6 scenario, and the RCP8.5 scenario. All warming patterns show a similar warming hole over the North Atlantic as for the observations (Fig. 1a), but the warming hole becomes less prominent when the radiative forcing gets stronger. It is most prominent in the historical run, and most weak in the RCP8.5 scenario. If the warming hole is caused by a decline of the AMOC, this suggests that the sensitivity of the AMOC for GMT change becomes weaker in a warmer climate. This is corroborated by the decreased regression of AMOC on GMT in more strongly forced scenarios, although the decrease is not significant (Table 1). Figure 1 also shows that the warming hole is larger in the observations than in the model ensembles.

By performing a bivariate regression, the pattern of GMT change can be decomposed into a pattern that is associated with the radiative forcing (assuming that this drives the GMT change in the RCP scenarios) and the fingerprint of the AMOC on SAT. Figure 2 shows that in the historical run the radiatively forced part still features a somewhat weaker warming hole, but in the RCP2.6 and other scenarios the warming hole is absent in the radiatively forced pattern. There, it is completely attributed to the AMOC fingerprint. This fingerprint has a pattern roughly similar to that of AMV, with warming over the North Atlantic associated with a positive AMOC anomaly (Figs. 2b,d). This result corroborates the hypothesis that the warming hole in the GMT trend pattern is caused by a decline of the AMOC.

At first sight, it may seem surprising that the warming hole is still part of the radiatively forced pattern in the historical runs. This could suggest that the separation between the radiatively forced pattern and the AMOC fingerprint is still incomplete. However, since
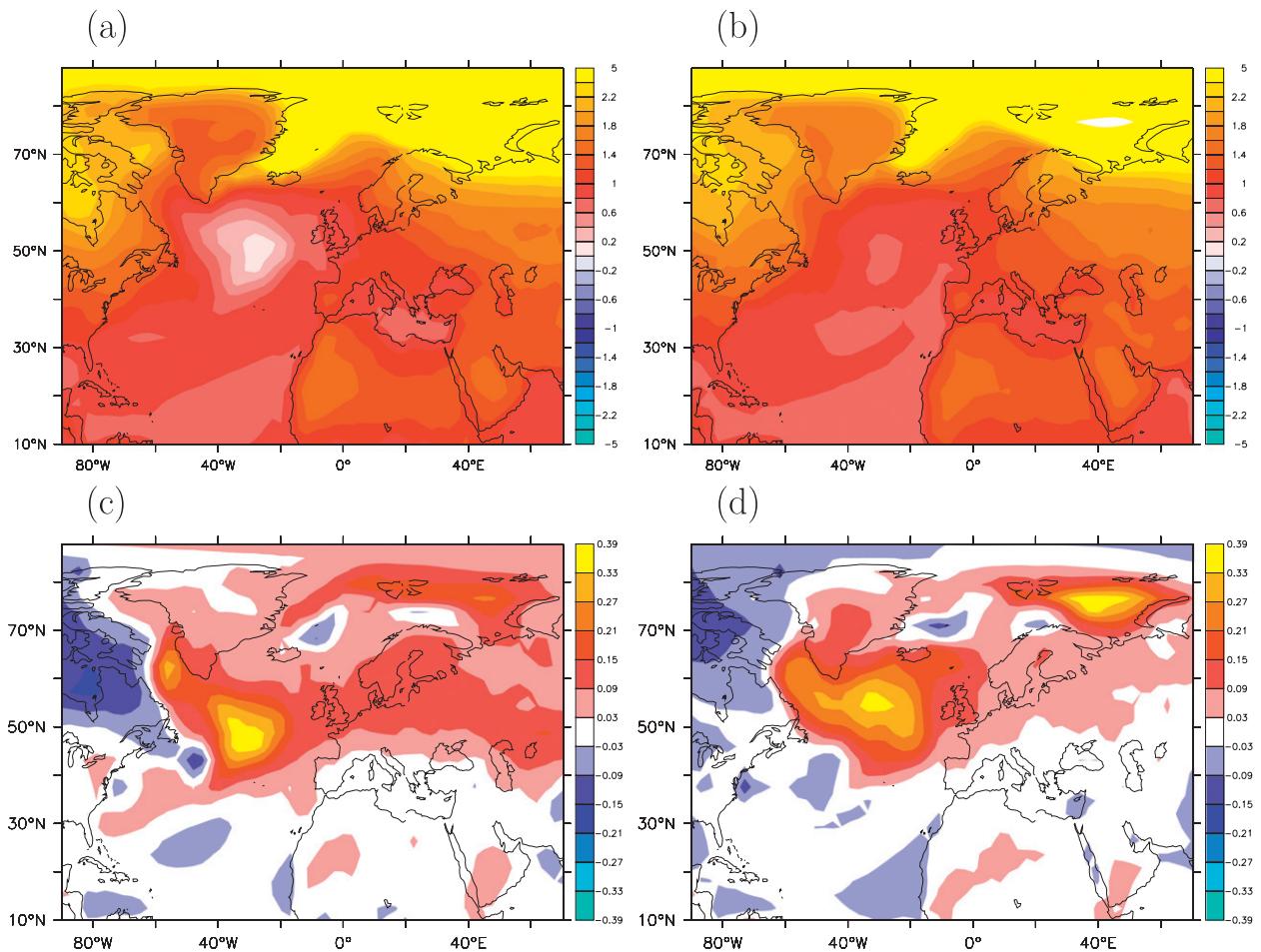
FIG. 2. Fingerprints obtained by a bivariate regression of SAT on GMT and an AMOC index, for the (a) radiative forcing fingerprint in the historical run, (b) radiative forcing fingerprint in the RCP2.6 scenario, (c) AMOC fingerprint in the historical run, and (d) AMOC fingerprint in the RCP2.6 scenario.

the response of the AMOC to GMT is small in the historical runs (Table 1) and GMT and AMOC are more weakly correlated than in the scenario runs (Table 2), a separation between the two patterns should work well for the historical runs. There must be another reason why the warming hole is less well associated with the AMOC in the historical runs. Several conjectures can be made to explain what is going on. One hypothesis is that the warming hole is part of an ocean adjustment that already precedes AMOC decline. In particular, in the RCP2.6 scenario the correlation between the warming hole and the AMOC increases, compared to the historical run, while the correlation between the warming hole and GMT becomes less negative (Table 2). This corroborates the hypothesis that the warming hole is partly forcing a lagged AMOC response. In the more strongly forced scenarios the correlation between the warming hole

and both GMT and AMOC increase further, as they both are dominated by a large monotonic trend. Note that these results do not change qualitatively when the AMOC index is derived from the maximum overturning; only the amplitude of the AMOC fingerprint is weaker in that case.

A second conjecture is that aerosols partly cause the warming hole in the historical runs. Since they have a stronger influence on the twentieth-century climate than on future projections, the warming hole could be part of the radiatively forced pattern in historical runs, while in the scenario runs it would be due to the AMOC. Whether aerosols do play a role in producing the North Atlantic warming hole remains unclear. For instance, Ming et al. (2011) found cooling over the midlatitude North Pacific due to aerosols, but found a weak diffusive signal over the North Atlantic. On the other hand, Booth et al. (2012) suggest a strong link between

TABLE 2. The correlation between GMT and the AMOC index, the warming hole and the AMOC index, and the warming hole and GMT for the CMIP5 model ensemble. The warming hole is defined as temperature averaged over 40°–20°W, and 45°–60°N minus temperature averaged over 45°–60°N. In this calculation the RCP scenarios were taken separately, and not joined with data from the historical period.

Scenario	AMOC/GMT	AMOC/WH	GMT/WH
Historical	−0.16	0.23	−0.50
RCP2.6	−0.61	0.57	−0.41
RCP4.5	−0.79	0.71	−0.67
RCP8.5	−0.90	0.87	−0.85

aerosols and the AMV. While there are too many unknowns in the historical aerosol forcing to unequivocally attribute SAT fingerprints to aerosol forcing, the possibility that aerosol forcing might be partly responsible for the warming hole in the historical period cannot be excluded.

A third conjecture is that the main driver for AMOC variability changes between the historical period and future scenarios. In the historical runs many AMOC variations may be associated with wind stress changes, while in the scenario runs the change in hydrological cycle might become the dominant driver for AMOC changes.

The warming hole is situated southeast of the deep convection sites in the Labrador and Irminger Seas, indicating that it cannot be interpreted as the passive SAT response to changes in deep convection. It must also involve changes in the subpolar gyre circulation, which would point to conjecture one. On the other hand, many climate models feature deep convection west of Ireland, associated with a too zonal North Atlantic Current (van Oldenborgh et al. 2009). However, both in the observations and in the CMIP3 ensemble the warming hole is situated south of the regions of maximum heat loss (Bitz et al. 2012), suggesting that it does not arise as a passive response to a decrease in deep convection.

The decrease of the warming hole for more strongly forced scenarios is not simply the expression for a decreased sensitivity of the AMOC to further GMT rise after GMT has increased. Although the regression of AMOC strength per degree GMT slightly changes, decreasing from the RCP2.6 to the RCP8.5 scenarios (Table 1), the decrease is not significant. An inspection of the differences between the patterns for the various scenarios reveals that the more strongly forced scenarios feature larger cooling in the Nordic seas (Fig. 3). This can be explained by the fact that in most models convection in the Labrador and Irminger Seas is more vulnerable to changes in external forcing, and that in general the Labrador and Irminger Seas first respond to

climate change, only followed by the Nordic seas when convection in the Labrador and Irminger Seas have nearly ceased (Wood et al. 1999; Drijfhout et al. 2008; Cheng et al. 2011). So, although the warming hole is not situated above the regions of maximum heat loss, there must be a link between the warming hole and changes in deep convection in the western part of the subpolar North Atlantic.

4. Summary and conclusions

We have investigated the GMT trend pattern in the observations and in CMIP5 models. The pattern was decomposed in a radiatively forced part and an AMOC fingerprint. The trend pattern obtained by regressing SAT on GMT contains a warming hole over the subpolar North Atlantic. By use of a bivariate regression we were able to demonstrate that the warming hole is associated with the AMOC; in the RCP scenarios the radiatively forced fingerprint does not contain the warming hole. The AMOC fingerprint in the RCP scenarios resembles the AMV (Latif et al. 2004; Knight et al. 2005; Dijkstra et al. 2006), corroborating the finding of Ottera et al. (2010) that phasing of the AMV can be paced by the external forcing, although details of the fingerprint change when forcing and AMOC decline become stronger.

The warming hole is situated southeast of the deep convection sites in the Labrador and Irminger Seas, which is once more a sign of the complex relation between convective overturning and the AMOC (Marotzke and Scott 1999; Pickart and Spall 1999). The fact that both observations and models show maximum cooling in the center of the subpolar gyre indicates that both subpolar gyre and AMOC adjust in concert, but with different time lags—a feature that has been discussed in various modeling studies (Eden and Willebrand 2001; Böning et al. 2006). A lagged adjustment to global warming of the AMOC, preceded by an adjustment of the subpolar gyre, is consistent with the warming hole being most prominent in the historical runs, where the AMOC decline per degree GMT is smallest. Other conjectures, however, also offer explanations for this feature. In the RCP scenarios the model ensemble captures an AMOC fingerprint that elucidates the observed warming hole, which is absent in the radiatively forced pattern. This strong connection is apparent in all scenarios where the AMOC is dominated by a downward trend. Model spread in fingerprint and response of the AMOC to GMT, however, is very large, underscoring the large uncertainty in AMOC projections for the next century (Reintges et al. 2012, manuscript submitted to *J. Climate*). When the radiative forcing becomes stronger, a robust increase of cooling over the Nordic seas arises, which is consistent with previous
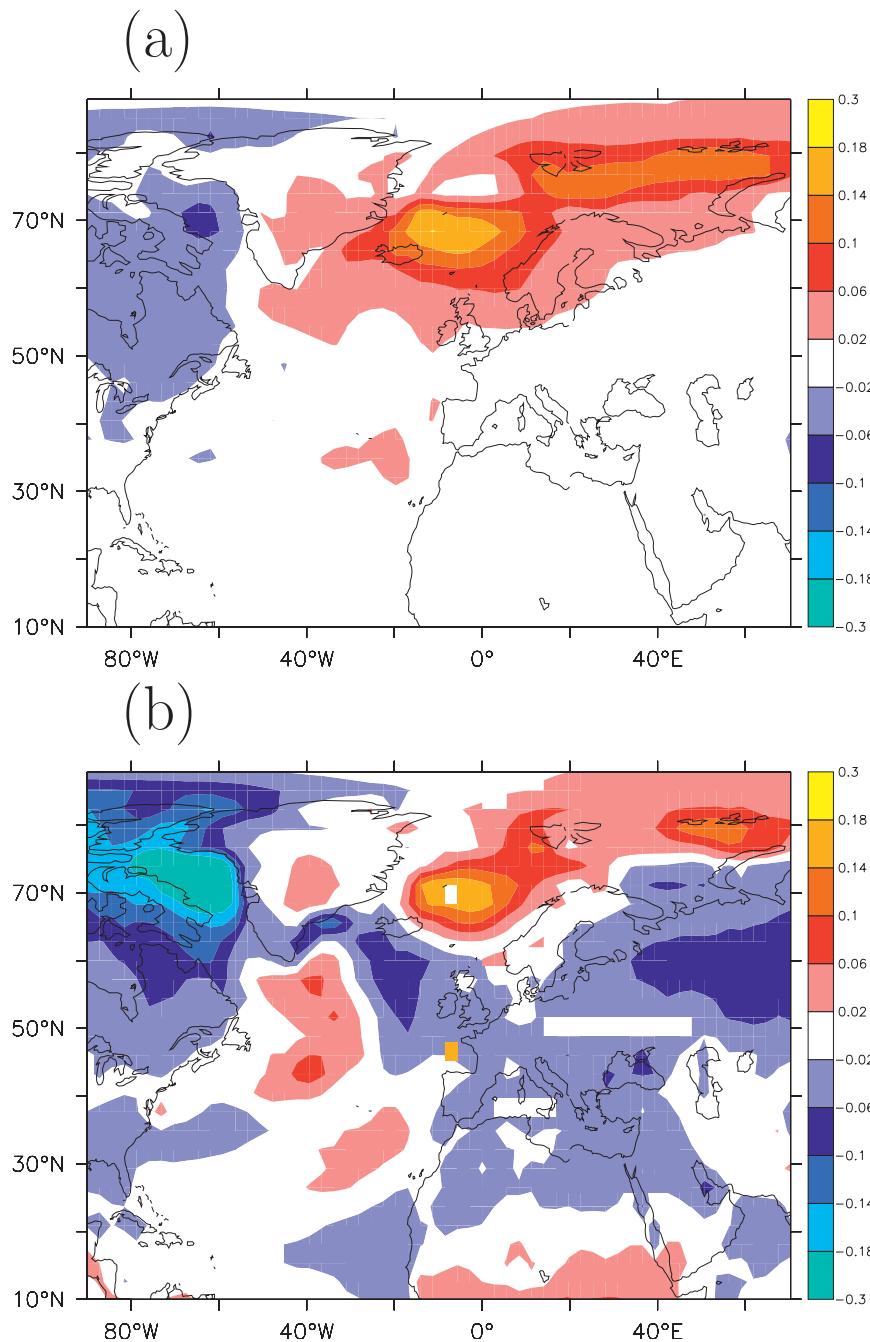
FIG. 3. Difference in AMOC fingerprints for the (a) RCP4.5 minus RCP2.6 scenario and (b) RCP8.5 minus RCP2.6 scenario.

findings that deep convection in the Labrador and Irminger Seas is more vulnerable to changes in external forcing, and that the convection in the Nordic seas only reacts to changes in external forcing after a threshold is passed, underscoring the nonlinearity of the AMOC response.

AMOC fingerprints in other measures than SAT have been promoted by Zhang (2008) and Mahajan et al.

(2011). It remains a challenge to investigate whether their fingerprints can be recovered from the CMIP5 ensemble applying the same technique as used here. Establishing the relation between the AMOC fingerprint on SAT, and other quantities, such as sea surface height, subsurface temperature, and upper ocean heat content, would enable a more dynamical understanding of how the subpolar warming hole arises in association with an AMOC decline.

Finally, we address whether the question posed in the title of this manuscript has been answered. With the present knowledge, we point to the case that all model results indicate that the warming hole is the precursor of an AMOC decline that is bound to occur in the coming century.

REFERENCES

Bitz, C., J. Ridley, M. Holland, and H. Cattle, 2012: 20th and 21st century arctic climate in global climate models. *Arctic Climate Change: The ACSYS Decade and Beyond,* P. Lemke and H.-W. Jacobi, Eds., Springer-Verlag, 405–436.

Böning, C. W., M. Scheinert, J. Dengg, A. Biastoch, and A. Funk, 2006: Decadal variability of subpolar gyre transport and its reverberation in the North Atlantic overturning. *Geophys. Res. Lett.,* **33,** L21S01, doi:10.1029/2006GL026906.

Booth, B. B. B., N. J. Dunstone, P. R. Halloran, T. Andrews, and N. Bellouin, 2012: Aerosols implicated as a prime driver of twentieth-century North Atlantic climate variability. *Nature,* **484,** 228–232.

Cheng, J., Z. Liu, F. He, L. Otto-Bliesner, and C. Colose, 2011: Impact of North Atlantic–GIN Sea exchange on deglaciation evolution of the Atlantic meridional overturning circulation. *Climate Past,* **7,** 935–940.

Dijkstra, H. A., L. A. Te Raa, M. Schmeits, and J. Gerrits, 2006: On the physics of the Atlantic multidecadal oscillation. *Ocean Dyn.,* **56,** 36–50, doi:10.1007/s10236-005-0043-0.

Drijfhout, S. S., and W. Hazeleger, 2007: Detecting Atlantic MOC changes in an ensemble of climate change simulations. *J. Climate,* **20,** 1571–1582.

——, ——, F. Selten, and R. Haarsma, 2008: Future changes in internal variability of the Atlantic meridional overturning circulation. *Climate Dyn.,* **30,** 407–419.

Eden, C., and J. Willebrand, 2001: Mechanism of interannual to decadal variability of the North Atlantic circulation. *J. Climate,* **14,** 2266–2280.

Hansen, J., R. Ruedy, M. Sato, and K. Lo, 2010: Global surface temperature change. *Rev. Geophys.,* **48,** RG4004, doi:10.1029/2010RG000345.

Knight, J. R., R. J. Allen, C. K. Folland, M. Vellinga, and M. E. Mann, 2005: A signature of persistent natural thermohaline circulation cycles in observed climate. *Geophys. Res. Lett.,* **32,** L20708, doi:10.1029/2005GL024233.

Latif, M., and N. S. Keenlyside, 2011: A perspective on decadal climate variability and predictability. *Deep-Sea Res. II,* **58,** 1880–1894.

——, and Coauthors, 2004: Reconstructing, monitoring, and predicting multidecadal-scale changes in the North Atlantic thermohaline circulation with sea surface temperature. *J. Climate,* **17,** 1605–1614.

Mahajan, S., R. Zhang, T. Delworth, S. Zhang, A. J. Rosati, and Y.-S. Chang, 2011: Predicting Atlantic meridional overturning (AMOC) variations using subsurface and surface fingerprints. *Deep-Sea Res. II,* **58,** 1895–1903.

Marotzke, J., and J. Scott, 1999: Convective mixing and the thermohaline circulation. *J. Phys. Oceanogr.,* **29,** 2962–2970.

Meehl, G., and Coauthors, 2007: Global climate projections. *Climate Change 2007: The Physical Science Basis,* S. Solomon et al., Eds., Cambridge University Press, 747–845.

Ming, Y., V. Ramaswamy, and G. Chen, 2011: A model investigation of aerosol-induced changes in boreal winter extratropical circulation. *J. Climate,* **24,** 6077–6091.

Msadek, R., and C. Frankignoul, 2009: Atlantic multidecadal oceanic variability and its influence on the atmosphere in a climate model. *Climate Dyn.,* **33,** 45–62.

Ottera, O. H., M. Bentsen, H. Drange, and L. Suo, 2010: External forcing as a metronome for Atlantic multidecadal variability. *Nat. Geosci.,* **3,** 688–694.

Pickart, R. S., and M. A. Spall, 1999: Impact of Labrador Sea convection on the North Atlantic meridional overturning circulation. *J. Phys. Oceanogr.,* **37,** 2207–2227.

Taylor, K. E., R. J. Stouffer, and G. A. Meehl, 2012: An overview of CMIP5 and the experiment design. *Bull. Amer. Meteor. Soc.,* **93,** 485–498.

van Oldenborgh, G. J., S. S. Drijfhout, A. P. van Ulden, R. Haarsma, C. Sterl, A. Severijns, W. Hazeleger, and H. A. Dijkstra, 2009: Western Europe is warming much faster than expected. *Climate Past,* **5,** 1–12.

Wood, R. A., A. Keen, J. Mitchell, and J. Gregory, 1999: Changing spatial structure of the thermohaline circulation in response to atmospheric CO_2 forcing in a climate model. *Nature,* **399,** 572–575.

Woollings, T., J. M. Gregory, J. Pinto, M. Reyers, and D. Brayshaw, 2012: Response of the North Atlantic storm track to climate change shaped by ocean–atmosphere coupling. *Nat. Geosci.,* **5,** 313–317.

Wouters, B., S. S. Drijfhout, and W. Hazeleger, 2012: Interdecadal North Atlantic meridional overturning circulation variability in EC-EARTH. *Climate Dyn.,* **39,** 2695–2712, doi:10.1007/s00382-012-1366-4.

Zhang, R., 2008: Coherent surface–subsurface fingerprint of the Atlantic meridional overturning circulation. *Geophys. Res. Lett.,* **35,** L20705, doi:10.1029/2008GL035463.